NUMERICAL INVESTIGATIONS IN THREE-DIMENSIONAL INTERNAL FLOWS

SEMI-ANNUAL STATUS REPORT

1 JULY THROUGH 31 DECEMBER 1990

Prepared for:

NASA-AMES RESEARCH CENTER

MOFFETT FIELD, CA 94035

UNDER NASA GRANT

NCC 2-507

By:

WILLIAM C. ROSE

ENGINEERING RESEARCH AND DEVELOPMENT CENTER

UNIVERSITY OF NEVADA, RENO

RENO, NV 89557

I. BACKGROUND

In 1990, NASA initiated its Generic Hypersonics Research Program. The general area of interest in this program is to develop a technology background for aeronautical research in the hypersonic Mach number flow range. Research efforts in the National Aerospace Plane (NASP) program have indicated limitations of numerical simulation techniques involving computational fluid dynamics (CFD). On the other hand, as part of NASA's NASP effort, the "Mach 5" inlet (References 1 and 2) that was designed for a flight Mach number of 5 has been built and successfully tested. Significant computational efforts have been expended in this effort and limited validation of some full three-dimensional Navier-Stokes codes has been obtained. However, the range of flow above Mach 5 is relatively uncharted, particularly with respect to the propulsion path components, and the inlet in particular. Previous experience in the NASP program has indicated that full three-dimensional Navier Stokes codes remain largely unvalidated for complex internal flow fields such as those arising in hypersonic inlets for the Mach numbers tested between about 7 and 22 (see, for example, References 3 and 4). In contrast to the three-dimensional codes, a two-dimensional code (SCRAM2D) has been validated for some two-dimensional hypersonic inlets (Reference 5) and has been proposed for use as a design tool due to its reasonable results, ease of use, and relatively short computer turnaround time.

The purpose of the present report is to describe the application of the SCRAM2D code to investigating the flow fields that might be expected to occur in a representative Mach 10, two-dimensional (ramp-compression) inlet.

II. INTRODUCTION

It is usually assumed, for vehicles operating in the atmosphere above Mach numbers of about 5, that the propulsion system must be a highly integrated portion of the overall vehicle. In addition, because of high-temperatures and the limitations of existing materials, control (such as bleed or injection) of the very thick viscous boundary layer entering the propulsion path as a result of the highly integrated forebody is expected to have limited practical application. Thus, it is desireable to develop the technology to rationally design an integrated inlet system that accepts (and deals with in the compression process) the entire forebody boundary layer. At higher Mach numbers this may be relatively easy due to the higher momentum content of the expected entering turbulent boundary layers. However, as the Mach number decreases, it is known that even the turbulent boundary layer becomes more liable to separation, and potential implications on inlet operability arise.

The purpose of the present investigation is to examine the behavior of a hypothetical two-dimensional (ramp-compression) inlet whose vehicle operating design Mach number for cruise applications has a value near 10. This Mach number was chosen because it represents a leap in the required technology above that employed in the Mach 5 inlet discussed previously. On the other hand, the Mach number of 10 is low enough so that gas-air chemistry issues, such as those associated with dissociation and ionization, are not expected to be the dominant issue in establishing the performance of the inlet. This Mach number allows the use of existing Navier-Stokes codes without the additional complexity of air chemistry and the associated large increases in computational time required to achieve numerical simulations of such flow fields.

Although the exact compression ratios and overall geometric turning angles that will be required for a given vehicle are not known in a generic sense, a representative inlet used for purposes of investigating the viscous behavior inside such an inlet has been chosen for this study. The CFD simulation consists of a two-dimensional inlet geometry that has an overall geometric turning of 36 degrees. It should be noted here that these simplistic geometric turning angles are not representative of the final compression ratio achieved by an inlet at high Mach numbers because of the large amount of additional compression related to the viscous displacement effects throughout the inlet. The 36 degree angle is achieved through an initial 10 degree pre-compression surface whose specific function is to increase the thickness of the boundary layer for this example inlet in order to produce a representative (and measurable) entering flow field to the remainder of the inlet. This is the initial ramp compression angle. Two other ramp deflections of 4 degrees each follow the initial 10 degree angle. Thus, the ramp produces an 18 degree turning angle up to the ramp shoulder. The cowl for this inlet is assumed to be aligned with the oncoming freestream flow, turning the ramp flow field back parallel to the freestream, thus producing the overall 36 degree turning angle. This arrangement is shown in Figure 1.

Because of the known dominant effect of the ramp boundary layer on the performance of the inlet, the cowl lip is positioned a distance of approximately 2½ times the ramp boundary layer thickness away from the ramp at the streamwise location of the cowl lip. This positioning of the cowl lip is actually a very stringent requirement since

most inlet studies assume that this ratio is at least 3. This choice of cowl positioning was made to illustrate the cowl shock wave-ramp boundary layer interaction effects that are the primary subject of the present investigation.

The particular geometry shown in Figure 1 has a straight cowl surface that is not contoured internally and the ramp shoulder has a radius transitioning from the 18 degree ramp surface to another straight surface that is parallel to the cowl. The ramp's leading edge is located at -1.5 m and the first 4 degree deflection is located at x = 0 m. The overall length is about 3.5 m, or about 11 feet. These representative inlet contours were derived based on previous CFD solutions using the SCRAM2D full Navier-Stokes code.

The following section describes the results of numerical simulations carried out at the design Mach number of 10 and two other off-design Mach numbers, 7.2 and 5.0. These Mach numbers are those available in the NASA-Ames Research Center's 3.5-ft hypersonic wind tunnel facility. The ultimate objective of this portion of the NASA Generic Hypersonics Program is to design, build and test an inlet model using the same philosophy as that embodied in the "Mach 5" inlet model. The "Mach 10" model would be capable of allowing variable geometry of an unprescribed nature to accommodate flow between the ranges of Mach number of 5 to 10, but having no bleed or injection. The following section discusses the results of the application of the SCRAM2D code, both at design and off-design conditions, using representative flow conditions available in the 3½-ft wind tunnel.

III. RESULTS AND DISCUSSION

III.1 Mach 10 Point-Design Studies

Typical results of a calculation for a given set of contours are shown using Figure 1's geometry in Figure 2. An understanding of the nature of the flow field within the inlet as portrayed in Figure 2 is essential to understanding the objectives of the present investigation. In order to elucidate these details, an entire multiple display of the results of the solution is given in Figures 2a through 2f. For the results discussed here, boundary layer has been assumed to undergo transition at a location of x = 0 meters on the ramp and on the cowl just downstream of the cowl lip. Figure 2a shows the Mach number contours obtained from the solution with a freestream Mach number of 10, superimposed on the geometry shown to the correct vertical and streamwise scales. All of the shock wave angles and geometrical positioning arrangements are accurate in this portrayal. In order to show the details of the solution, the vertical scale is expanded in Figure 2b, in which the boundary layer on the ramp, the cowl shock wave, the interaction of the ramp boundary layer and the cowl shock wave near the inlet shoulder, and the remaining viscous flow throughout the internal portion of the inlet are seen more clearly. Because of the expansion of the vertical scale, the shock wave angles are not accurate in this figure. A relatively strong interaction between the cowl shock wave and the ramp boundary layer is shown. An enlargement (also having an expanded vertical scale) of the flow just upstream of the cowl lip and the remainder of the inlet is shown in Figure 2c. Again, the Mach number contours are the flow variable being displayed and the strong effect of the cowl shock wave on the ramp boundary layer is evident. The location and displacement away from the ramp of the sonic line (M=1)

in the region of interaction of the cowl shock wave with the ramp boundary layer give an indication as to the effect of this interaction and the potential for problems in inlet operability (unstart) to arise. The larger the amount of subsonic flow in the inlet, the more likely downstream pressure gradients are to produce undesirable effects, including inlet unstart. Whenever a significant amount of subsonic flow exists within an interaction, such as that depicted in Figure 2c, a region of reverse flow, that is boundary layer separation, is likely to occur. However, the mere existence of boundary layer separation, in terms of inlet operability, is not an issue per se, since it is known that inlets can operate with small regions of separation. Other issues, such as the increase in surface heating expected to occur in these local regions of separation, may cause a modification to an inlet design, but they are not considered in the present study.

The Mach number contours in Figure 2c indicate a region of acceleration of the flow outside the viscous region just downstream of the ramp boundary layer-cowl shock wave interaction. This region is more clearly portrayed in a contour plot of the non-dimensionalized static pressures shown in Figure 2d. The near-field expansion was discussed briefly in Reference 3. This expansion is discussed further when surface pressure distributions are shown. This expansion arises not because of the geometric turn in the ramp from its 18 degree value back parallel to the cowl, but rather it is specifically associated with the imposition of a constant turning angle due to the cowl shock wave through a vortical flow of decreasing Mach number (the ramp boundary layer). This near-field interaction phenomenon, coupled with the difficulty of precisely positioning the cowl shock wave at a shoulder (due to the thickness of the ramp

boundary layer), precludes the ideal shock cancellation concept envisioned in so many hypersonic inlet research efforts. All turbulent boundary layer-shock wave interactions possess this local expansion region, and it is only the strength and geometric extent of the expansions that make this phenomenon important in the context of the present hypothetical inlet. In the far field of this interaction, the reflected shock wave (if present) encroaches into the expansion field, thus eliminating any trace of the expansion a long distance from the interaction. For presently conceived hypersonic inlet arrangements having very thick boundary layers associated with the integrated forebody inlet flow field, this near-field phenomenon must be dealt with. Experimental tests of arrangements similar to that discussed in Figures 1 and 2 have shown a train of oblique shock waves within the constant area portion of the inlet. The effects of the expansion and non-cancelled reflecting shock wave system can be seen in the pressure contours of Figure 2d and the surface pressure information depicted in Figures 2e and 2f. If these two curves are overlaid, a "ringing" phenomenon characteristic of the train of expansions and oblique shock waves can be clearly seen. The source of the expansion train is the near-field interaction effect discussed above. It is clear that this effect predominates the internal portion of the flow.

The solution shown in Figure 2 was obtained, of course, with the full Navier-Stokes code and contains all of the viscous effects associated with the boundary layers on the ramp and cowl surfaces. Although the overall pressure rises required for acceptable engine performance would be established from the vehicle mission requirements, the actual geometric flow turning angles in the inlet that might be required

are unknown in the presence of the dominant effect of the viscously induced aerodynamic turning that is illustrated by the results shown in Figure 2. In order to demonstrate the large influence that the viscous flow has on a simple configuration such as that shown in Figure 2, the inviscid solution shown in Figure 3 was obtained. In this solution, virtually no aspect of the design goals is met since the location and strength of the oblique shock wave system does not behave anything like that indicated by the use of the full Navier-Stokes code.

Potential methods for eliminating, or at least reducing the magnitudes of the pressure excursions that the internal boundary layers would be subjected to are of interest in this study. The following discussion centers about modifications of the cowl and ramp surfaces aimed at minimizing the effects of the near-field expansion and producing a more nearly ideal cancelled cowl shock wave.

One modification of the cowl and ramp geometry studied here is shown in Figure 4. Only the detailed portion of the flow field is shown, since the upstream flow is identical to that depicted in Figures 2a and 2b. For this geometry (denoted as Mod. 26), the cowl has been contoured in order to produce a compressive flow field at the location where the expansion from the ramp boundary layer-cowl shock wave interaction is expected to occur at the cowl surface. The intent of this contouring is to cancel the expansion. The cowl surface must ultimately turn back parallel to the freestream so that the remainder of the contour results in an "S-type" contour. The ramp has also been contoured to allow a nearly constant area duct to occur in the presence of the

contoured cowl. This amounts to overturning the ramp surface from its 18 degree compressive value to a value of about 5 degrees away from the originally aligned cowl surface. This turning of the ramp surface is expected to have a beneficial effect since it can reduce the strength of the pressure rise associated with the cowl shock wave and, thus, provide more margin against boundary layer separation at the ramp shoulder, which would ultimately provide more margin against inlet unstart. The ramp must also be turned back parallel to the cowl, resulting in the remaining geometry as depicted in Figure 4. Figure 4a shows the calculated Mach number contours for this inlet. Large differences between the Mach number contours of Figure 2c and Figure 4a are not immediately evident, however, when the pressure contours are compared, as in Figures 4b and 2d, a substantial change is evident. The cowl and ramp contouring tends to reduce the effect of the near-field expansion and minimize the strength of the reflected shock wave coming from the ramp surface. The surface pressure distribution information from the ramp and cowl is shown in Figures 4c and 4d respectively. These latter two figures show an improvement over the distributions depicted in Figures 2e and 2f. Pressure amplitude variations are much lower and this is beneficial in that the boundary layers on the ramp and cowl are not continually subjected to regions of strong adverse pressure gradient and the resulting loss of momentum associated with these compressions.

The inlet contours and the resulting solution depicted in Figure 4 are important because they indicate the possibility of modifying the contours, at least in a point design, to ameliorate the effect of the shock system and boundary layer effects exhibited by uncontoured solutions. Although the geometry portrayed in Figure 4 does not necessarily represent a good operating inlet, it does represent the possibility that inlets can be

designed to minimize adverse pressure gradient effects within the internal flow portion of the inlet. Again, for comparative purposes, the geometry shown in Figure 4 was solved using an inviscid code and results are shown in Figure 5. As with the simple geometry discussed in Figures 2 and 3, the results shown in Figure 5 indicate that inviscid codes are of little value.

Many other solutions have been obtained in the course of the present study, and a few of those are discussed in the following section to give the reader the flavor of the study conducted to date. In obtaining the numerous solutions, the SCRAM2D code was demonstrated to be a useful tool in a design environment accepting parametric variations of the geometry and returning the solutions in a useful time (15 min. Cray Y-MP single processor).

III.2 Off-Design Studies

The nature of the off-design Mach number issue can be demonstrated through the use of Figures 6 and 7. In these figures, the geometry used in Figures 1, 2 and 3 has been used to calculate the flow properties at off-design Mach numbers of 7.2 and 5.0. These solutions are for conditions representative of those available in the Ames 3½-ft wind tunnel. At the mid-range Mach number, the boundary layer does not appear to be substantially altered from that depicted in Figure 2, however, at Mach number of 5 a very large region of low Mach number flow is seen and is accompanied by a large region of reverse flow. This solution culminated in an unstart at Mach 5 when calculations were continued beyond those shown in Figure 7.

In order to determine whether or not various manipulations of the geometry can produce an acceptable flow field over the range of desired Mach numbers characterized by the solutions obtained at Mach 5, 7.2 and 10, the following sequence of modifications was attempted. Recall that the ramp boundary layer was separated by the cowl shock wave well ahead of the ramp's contoured shoulder (Figure 7). In order to determine if this separation could be eliminated by simply retracting the cowl lip, another solution was run, the results of which are shown in Figure 8. Even though the pressure rise on the ramp due to the cowl shock would be expected to occur well downstream of the ramp shoulder, the ramp boundary layer separates and, later, the inlet unstarts. The fundamental difficulty with this class of 36 degree inlets is that the shock wave from the cowl (which is aligned with the freestream) is too strong for the ramp boundary layer to maintain attached flow. This is a well-known problem and the following geometry changes are examined to determine if variable geometry can alleviate this problem.

To reduce the strength of the cowl shock wave, the second 4 degree ramp turn was eliminated. This produces an inlet whose geometric turning angle has a total of 28 degrees. The solution for this inlet at Mach 5 is shown in Figure 9 and indicates that, even though the cowl shock is reflected ahead of the ramp shoulder, the ramp boundary layer remains relatively well-behaved and the inlet operates without evidence of unstart. The overall compression ratio produced by this arrangement, of course, is much lower than the previous inlets due to the decrease of 8 degrees in geometric turning.

Another type of variable geometry was considered in which the angle downstream of the ramp shoulder was adjusted to tailor the ramp surface pressure gradient associated with the cowl shock wave-ramp boundary layer interaction. To investigate whether or not this concept is at all feasible, a geometry was generated which has an initial 10 degree turn away from the cowl surface. This geometry (Mod. 12F) was implemented and flow field results for a solution in which the cowl remained in the forward position is shown in Figure 10. In spite of the fact that the exit area of the throat remains large, the 10 degree expansion is insufficient to control the boundary layer separation when the cowl is in the forward position. This study shows that the cowl shock wave position is critical, and even a 10 degree geometric expansion at the ramp shoulder is insufficient to provide relief from the cowl shock wave pressure rise for the 36 degree inlet configuration.

Because of the recognized criticality of the cowl shock position, the entire cowl was retracted in another geometry (Mod. 12D) and the solution for Mach 5 is shown in Figure 11. With the retracted cowl, the inlet operates with a very small separation located near the shoulder. Some beneficial effects of the cowl contouring (which is actually the Mach 10 point design cowl from Figure 4) are seen from this solution. A question exists as to whether an inlet operating with a relatively large expansion in the throat region can be made to produce enough compression when the flow is recompressed in the internal flow portion of the inlet downstream of the throat. A geometry was generated which contains an additional internal contraction. The solution for this geometry (Mod. 12H) is shown in Figure 12. Indications here are that the

contoured ramp surface is capable of modifying the pressure gradient behavior sufficiently to allow a full 36 degree compression inlet to operate; however, the contouring is critical.

One final variable geometry concept was tried with the 18 degree ramp turning geometry based on the uncontoured geometry discussed in Figure 7. The cowl was allowed to pivot about a hypothetical hinge located near the expansion expected from the near-field effect discussed above. The cowl "droop" was 5 degrees to significantly reduce the strength of the cowl shock wave. Results from the calculation of this flow are shown in Figure 13 and indicate a successful operating inlet at Mach 5. Although this configuration potentially has a large unwanted cowl drag contribution, the trade-off at low Mach numbers must be made to assess its practicality.

Even though these hypothetical geometries are not intended to represent real variable geometry inlet designs, they do indicate the potential for modifying the pressure gradient history for the boundary layers on both ramp and cowl in order to produce an operating inlet with a relatively high final compression ratio. How these geometries might be envisioned to operate is discussed next.

III.3 Realization of the Variable Geometries

Geometric modifications investigated to date in the present study have shown the potential usefulness for positioning the cowl lip, contouring the cowl, and contouring the ramp in order to tailor the overall pressure gradients within the inlet. Variable geometry of some nature would appear to be necessary in order to allow the hypothetical type of inlet being discussed here to operate over the range of Mach numbers between 5 and 10.

Initially, if the 28 degree turning inlet with the contraction ratio similar to that investigated here were adequate for purposes of the Mach 5 operation, then additional compression would be obtained at the higher Mach numbers by simply providing a "pop-up" ramp with an additional 4 degree turning that would produce the 36 degree inlet tested here. This concept* appears to be viable, and would be relatively easy to implement.

In addition to the "pop-up" concept, the new concept of a drop-down throat, causing a geometric expansion to exist downstream of the ramp shoulder, has been investigated. Although perhaps more difficult to implement, since that concept must also prescribe the recompression process in the downstream portion of the internal flow, it appears to represent a viable candidate.

The cowl "droop" or variable angle portion of the cowl surface has a high payoff in controlling separation of the ramp boundary layer, but practical issues of cowl drag must be considered in the context of the desired mission.

*First suggested to the present authors by Bobby Sanders of NASA-Lewis.

IV. CONCLUDING REMARKS

The present study has conducted a preliminary investigation into the behavior of the flow within 36 degree and 28 degree total turning hypothetical inlet geometries. During the course of the study, numerous flow solutions were obtained using a full Navier-Stokes code in a design-type environment. The study has demonstrated the usefulness of this code to allow parametric modifications of the geometry in order to derive successful variations that meet the design objectives. Short run times allow "man-in-the-loop" interaction to occur rapidly enough to be practical in the design process.

Successful tailoring of the geometry at the inlet's shoulder and on the cowl have demonstrated the feasibility of using curved internal contours to allow the pressure gradients to be modified to meet certain objectives. The first objective is to produce an operating inlet that will not be prone to an inlet unstart. The second objective is to produce a flow field downstream of the ramp shoulder that has a minimum of expansions and compressions in the throat section of the inlet. These objectives have been met by contouring the ramp and cowl surfaces.

Although none of the configurations investigated here are proposed for actual inlet model designs, the investigation has demonstrated the requirement for some variable geometry concept to allow an inlet to operate throughout the range of Mach numbers between 5 and 10. Three candidate variable geometry concepts were investigated here and shown to alleviate separation of the ramp boundary layer by the cowl shock wave.

Much of the present investigation centers around the predominant viscous effects in the inlet. Although the SCRAM2D code used here has been validated in similar flow fields, the effects of full 3D flows (associated with sidewalls, for example) have not been considered here. Because the weakest point in the present CFD validations is in predicting the details of separated flow, experiments are required to verify the current predictions.

V. REFERENCES

1. Perkins, E.W., Rose, W.C., and Horie, G: Design of a Mach 5 Inlet System Model, NASA CR-3830, August 1984.

2. Weir, L.J., Reddy, D.R., and Rupp, G.D.: Mach 5 Inlet CFD and Experimental Results. AIAA Paper 89-2355, July 1989.

3. Rose, W.C., Perkins, E.W., Bencze, D.P. and Howe, G.W.: Comparison of CFD Results and Experimental Data for Scramjet Inlet at M=8 and 18. Paper presented at the 7th NASP Technology Symposium, October 1989.

4. Rose, W.C., Perkins, E.W., Howe, G.W., and Bencze, D.P.: Analysis of the Flow in Sidewall Comparison Inlet at Hypersonic Mach Numbers. NASP Contractor Report 1064, October 1989.

5. Rose, W.C. and Perkins, E.W.: Towards Establishing Full Navier-Stokes Simulations as Design Tools for High-Speed Inlets. Prepared for NASA-Lewis NASP Quick Release CR. April 1990.

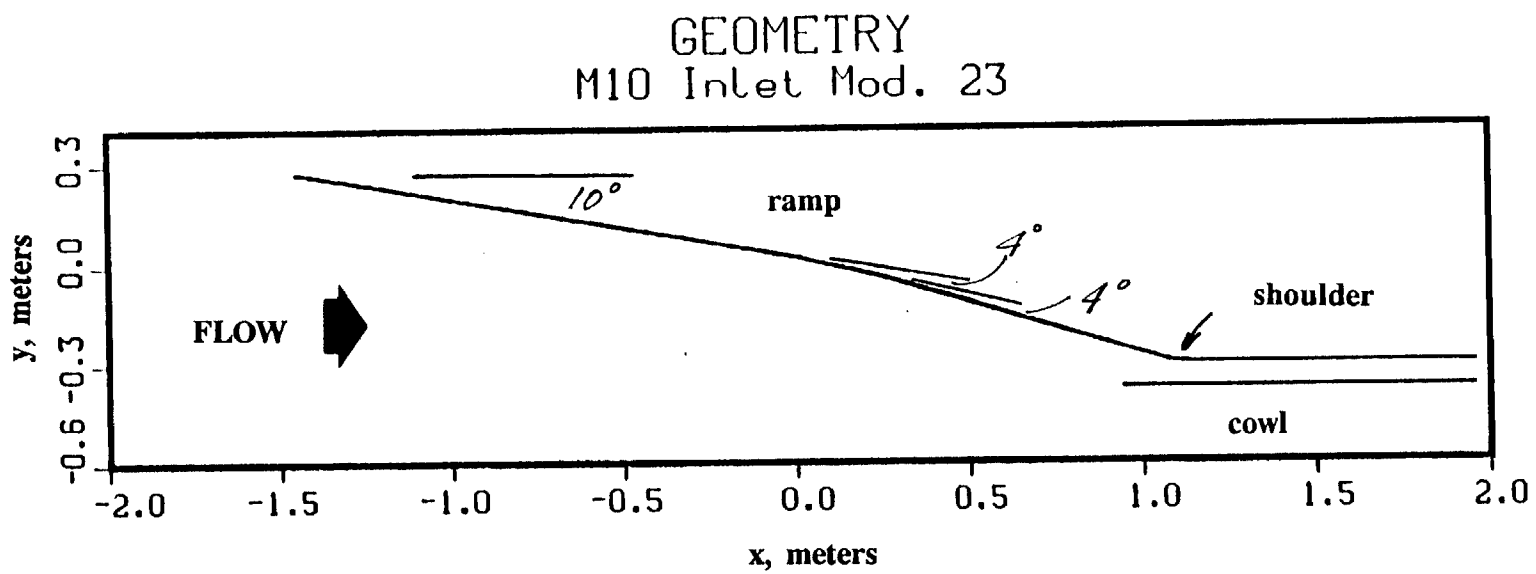

FIGURE 1. **Geometry for 36 degree inlet having a straight cowl and straight ramp.**

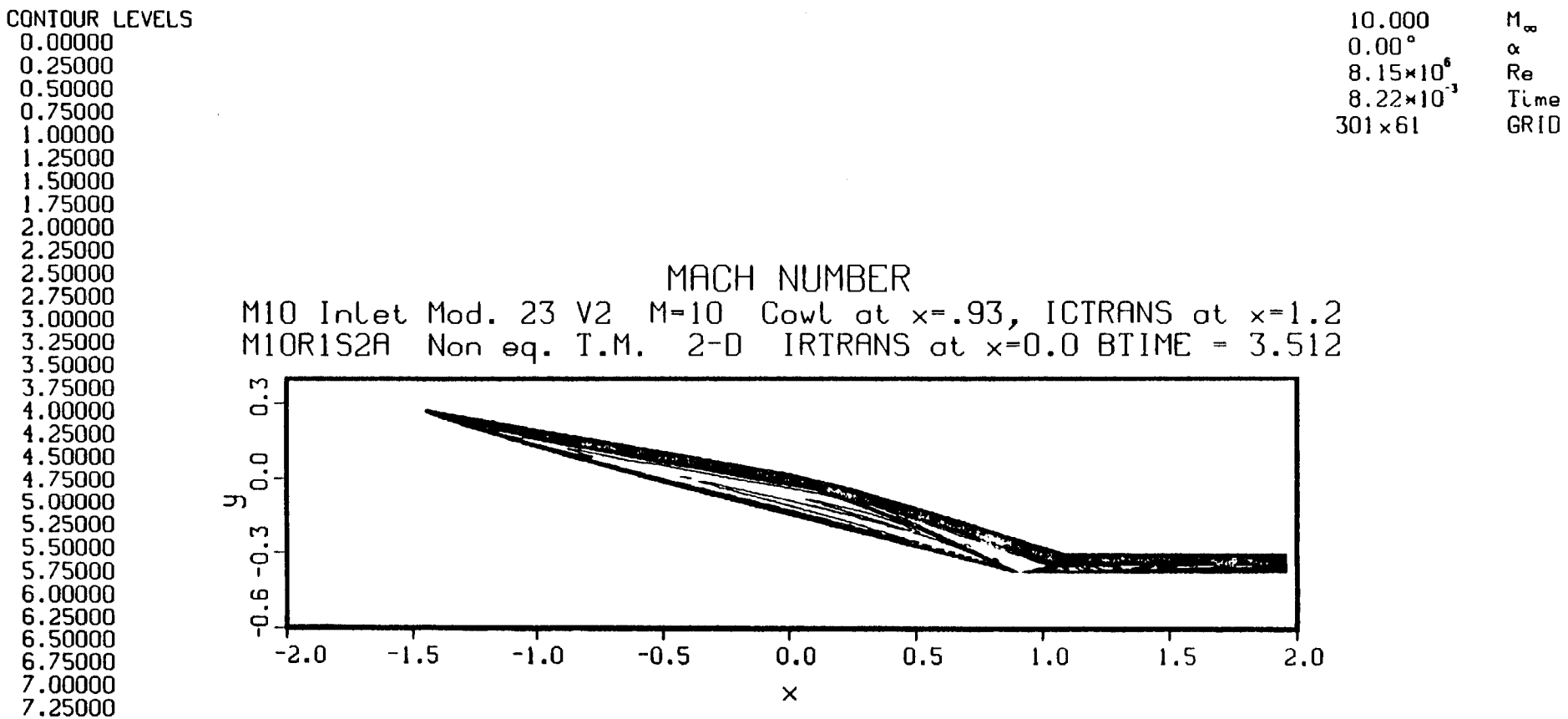

FIGURE 2. **Flow solution for 36 degree inlet with straight ramp and cowl at M = 10.**

(a) Mach number contours shown to correct vertical and streamwise scales.

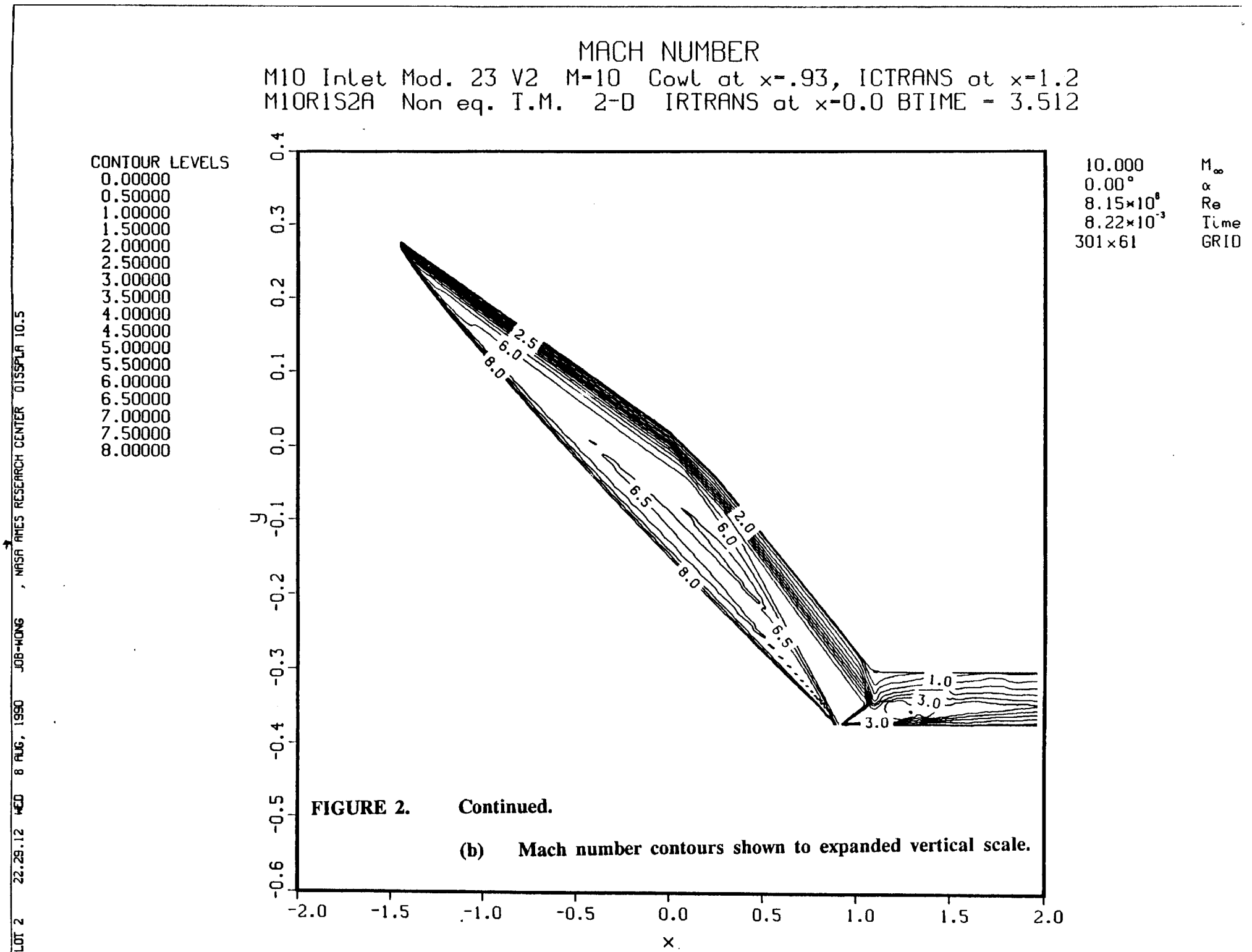

FIGURE 2. **Continued.**

(b) Mach number contours shown to expanded vertical scale.

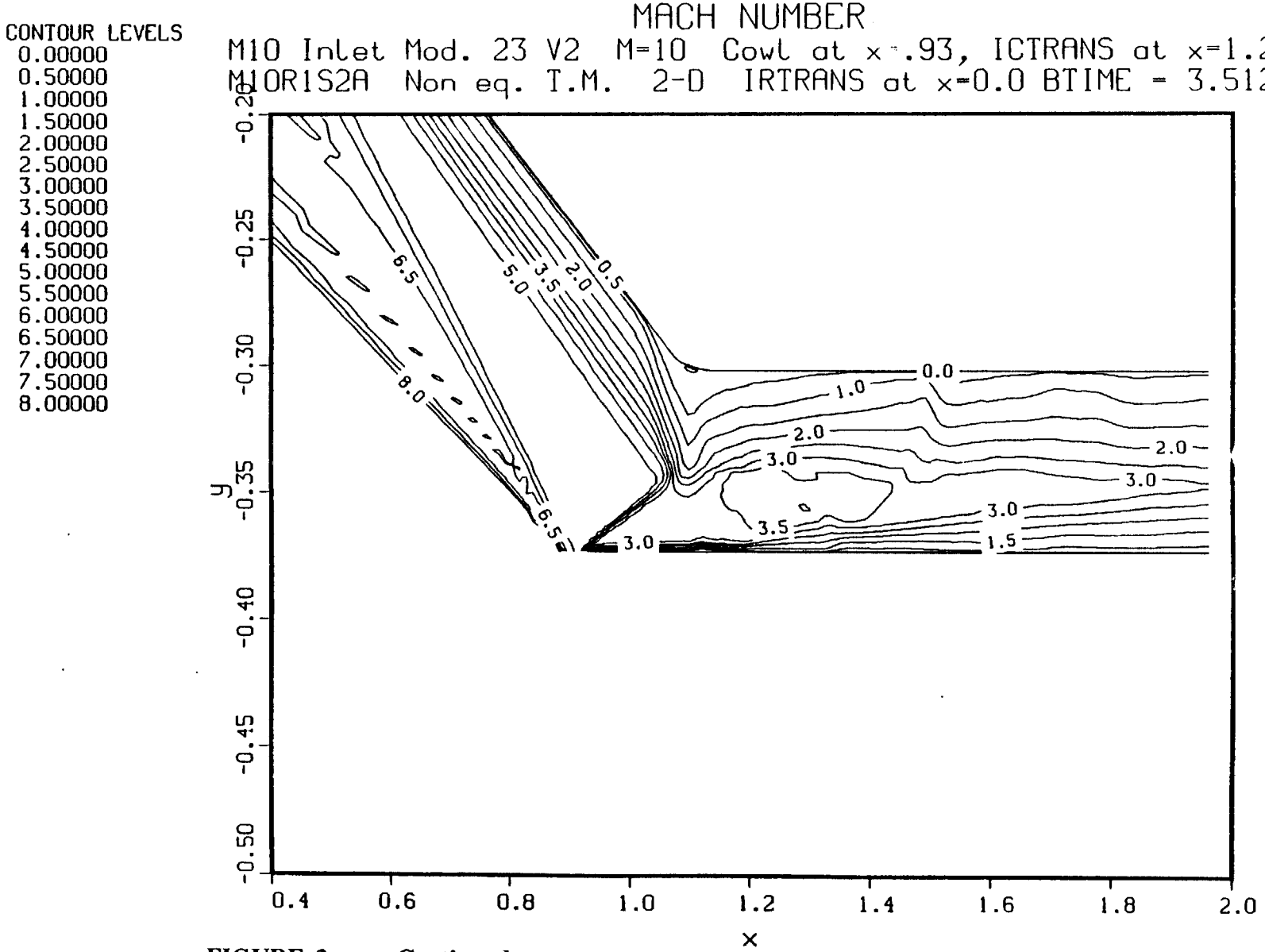

FIGURE 2. **Continued.**

(c) **Mach number contours shown enlarged to indicate detail in throat region.**

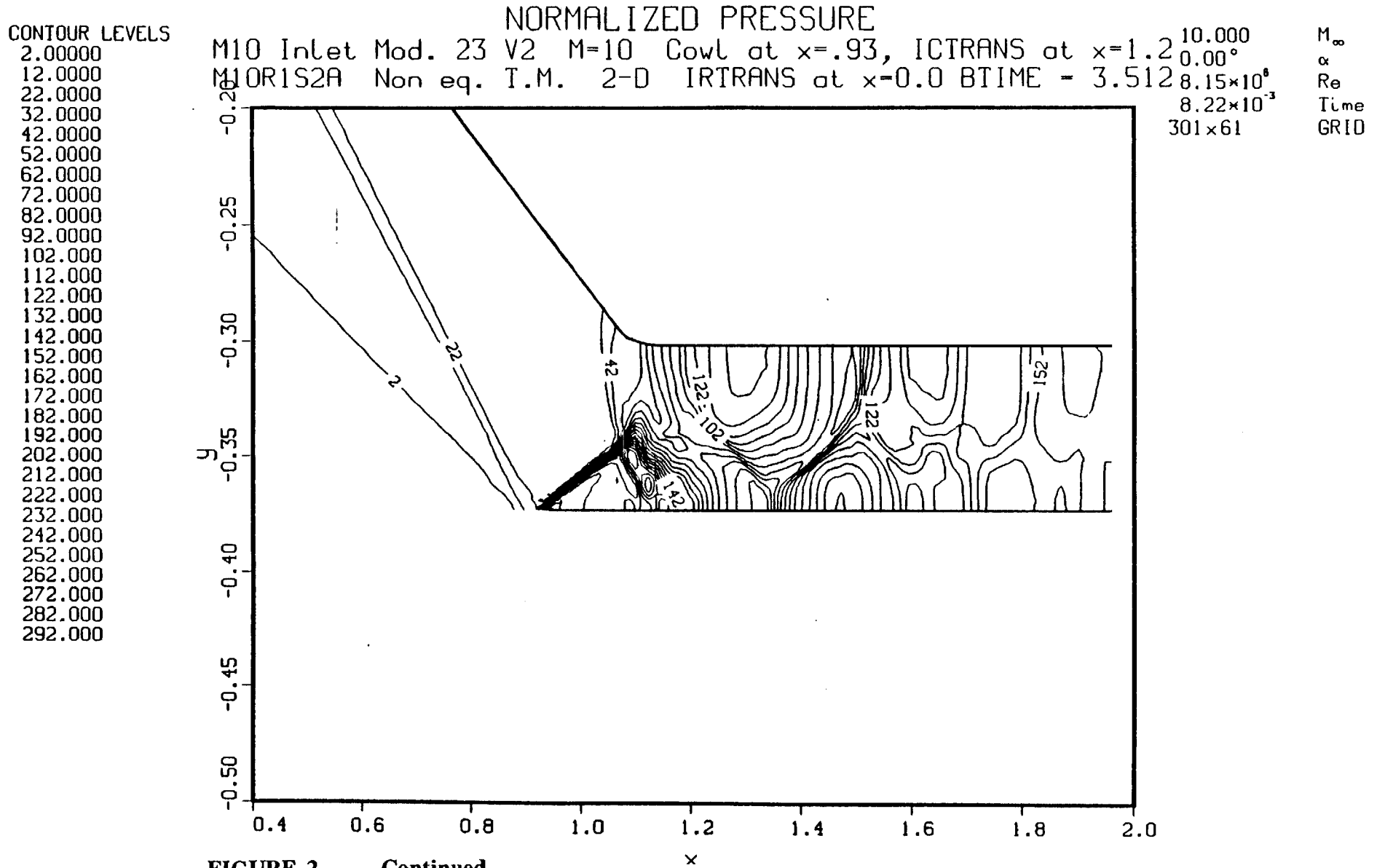

FIGURE 2. Continued.

(d) Pressure contours in throat region.

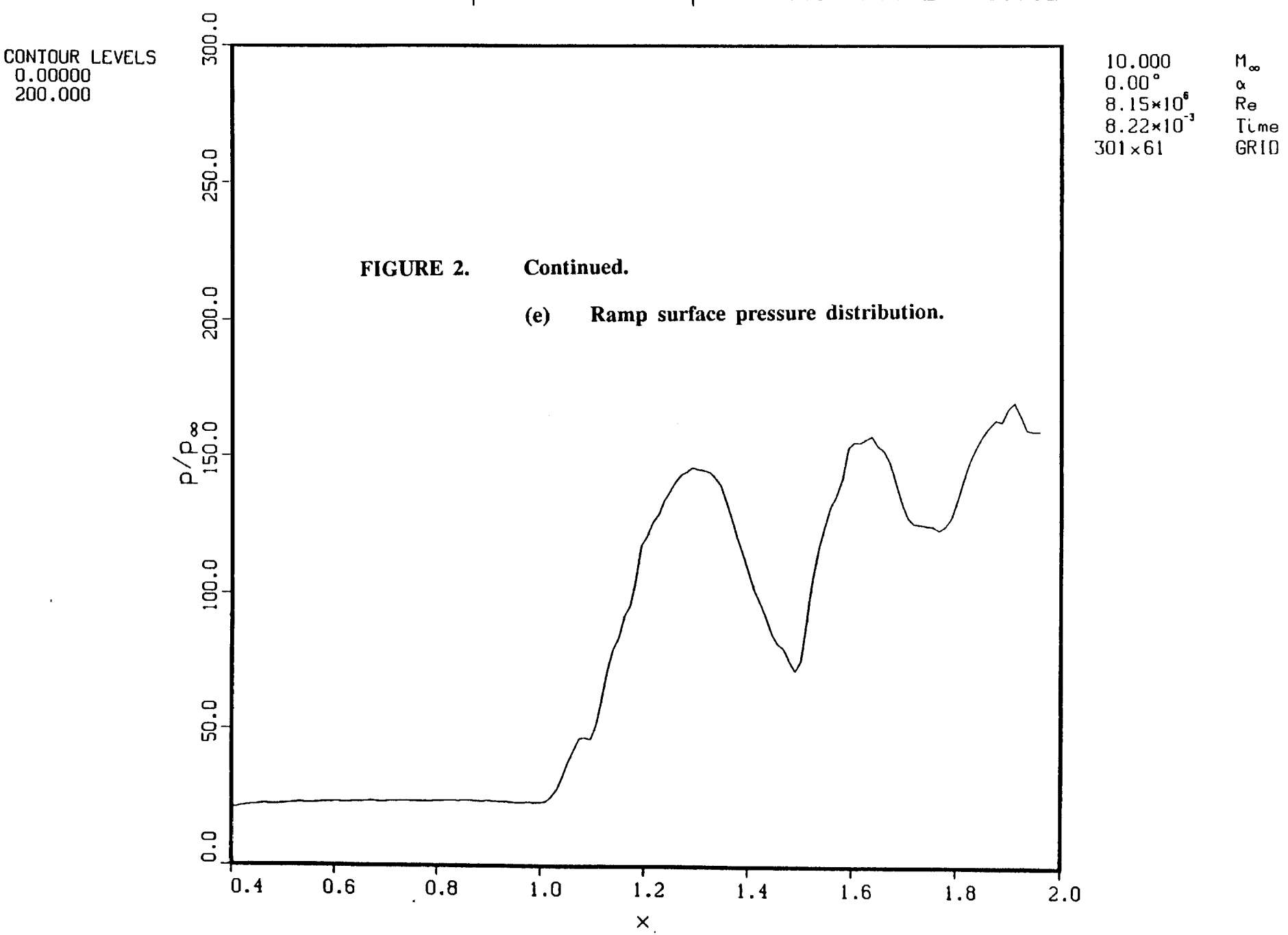

FIGURE 2. Continued.

(e) Ramp surface pressure distribution.

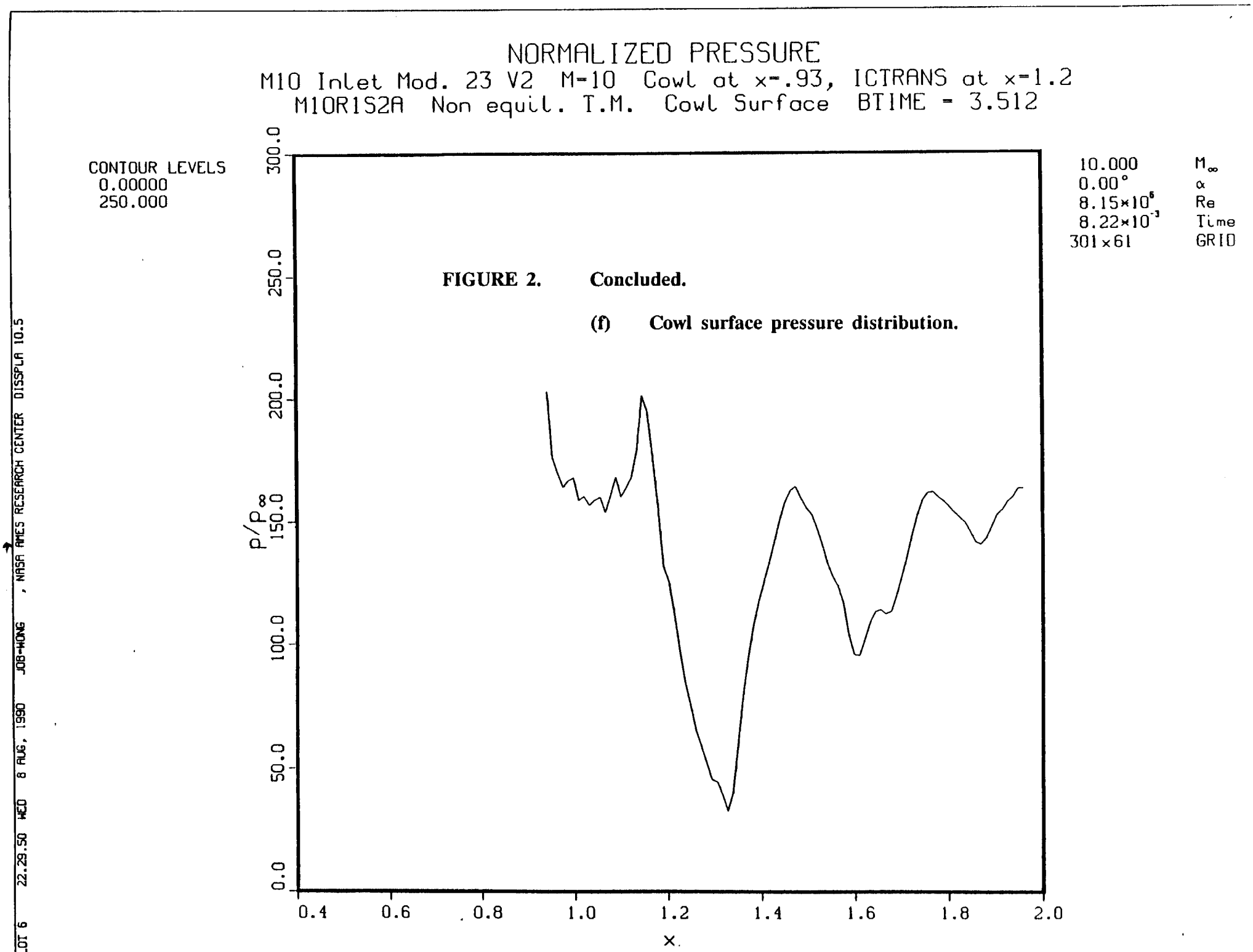

FIGURE 2. Concluded.

(f) Cowl surface pressure distribution.

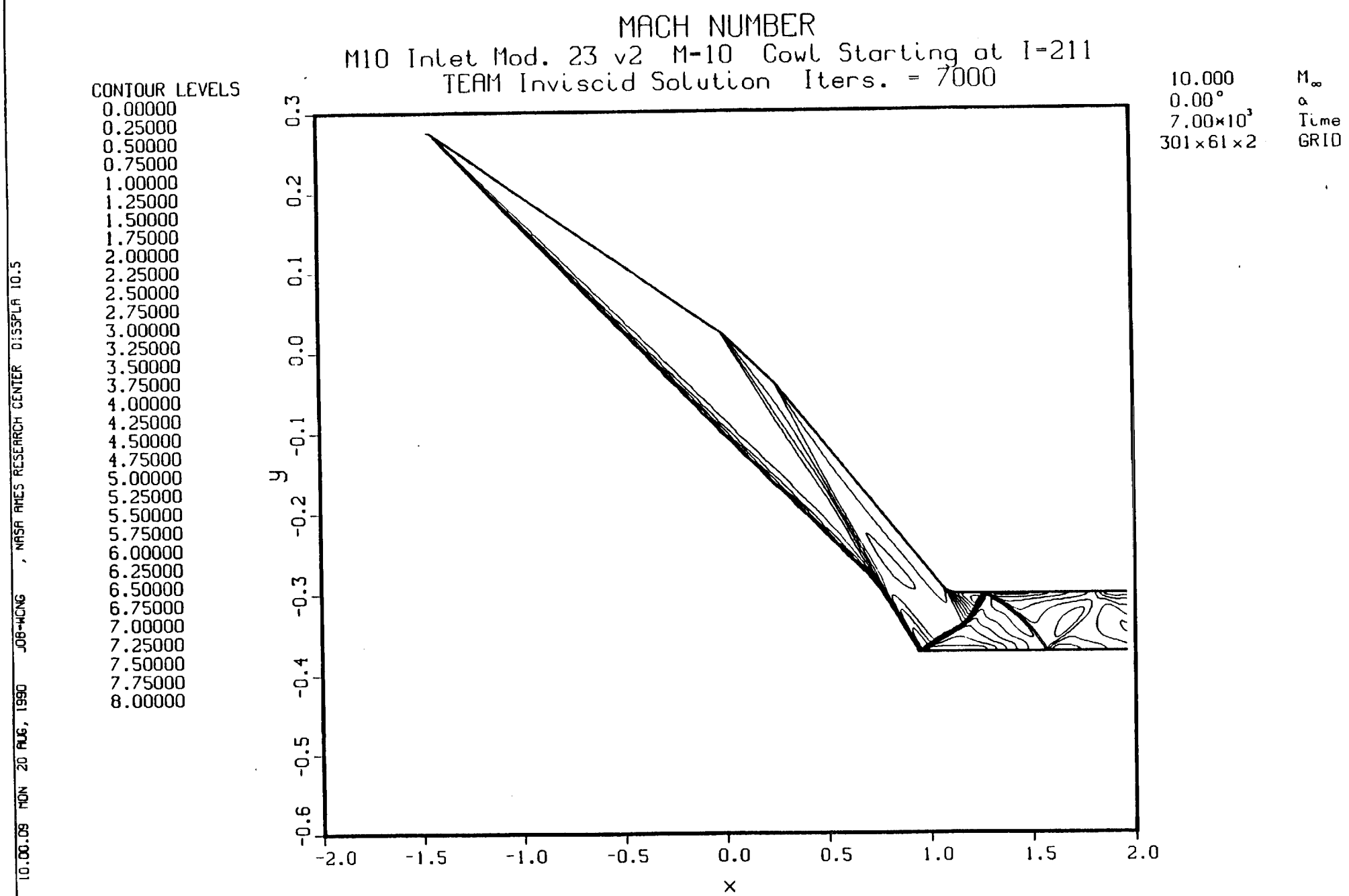

FIGURE 3. Inviscid flow solution for the inlet with straight ramp and cowl at M=10.

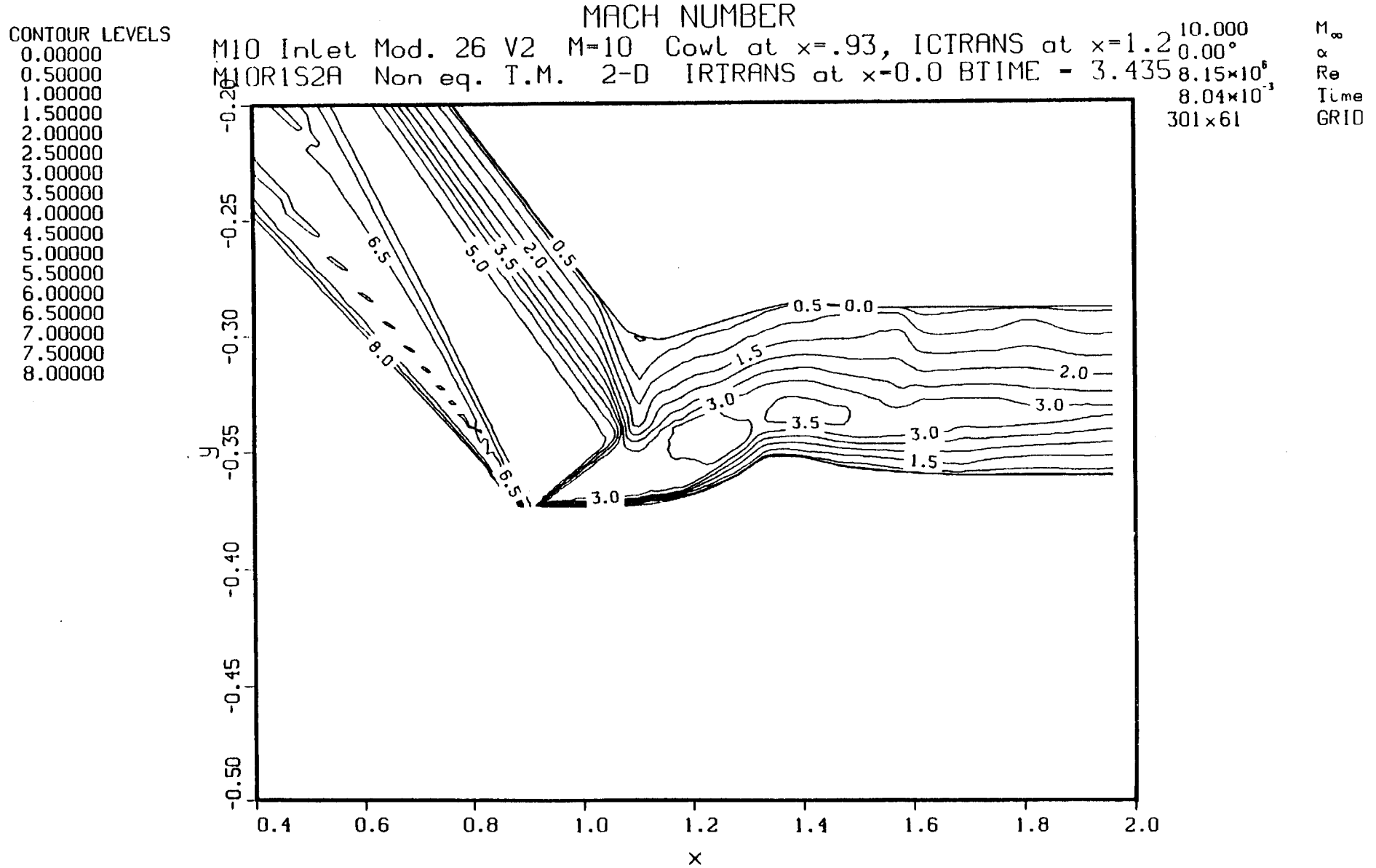

FIGURE 4. **Flow solution for 36 degree inlet with contoured ramp and cowl surfaces at M = 10.**

(a) Mach number contour detail in throat region.

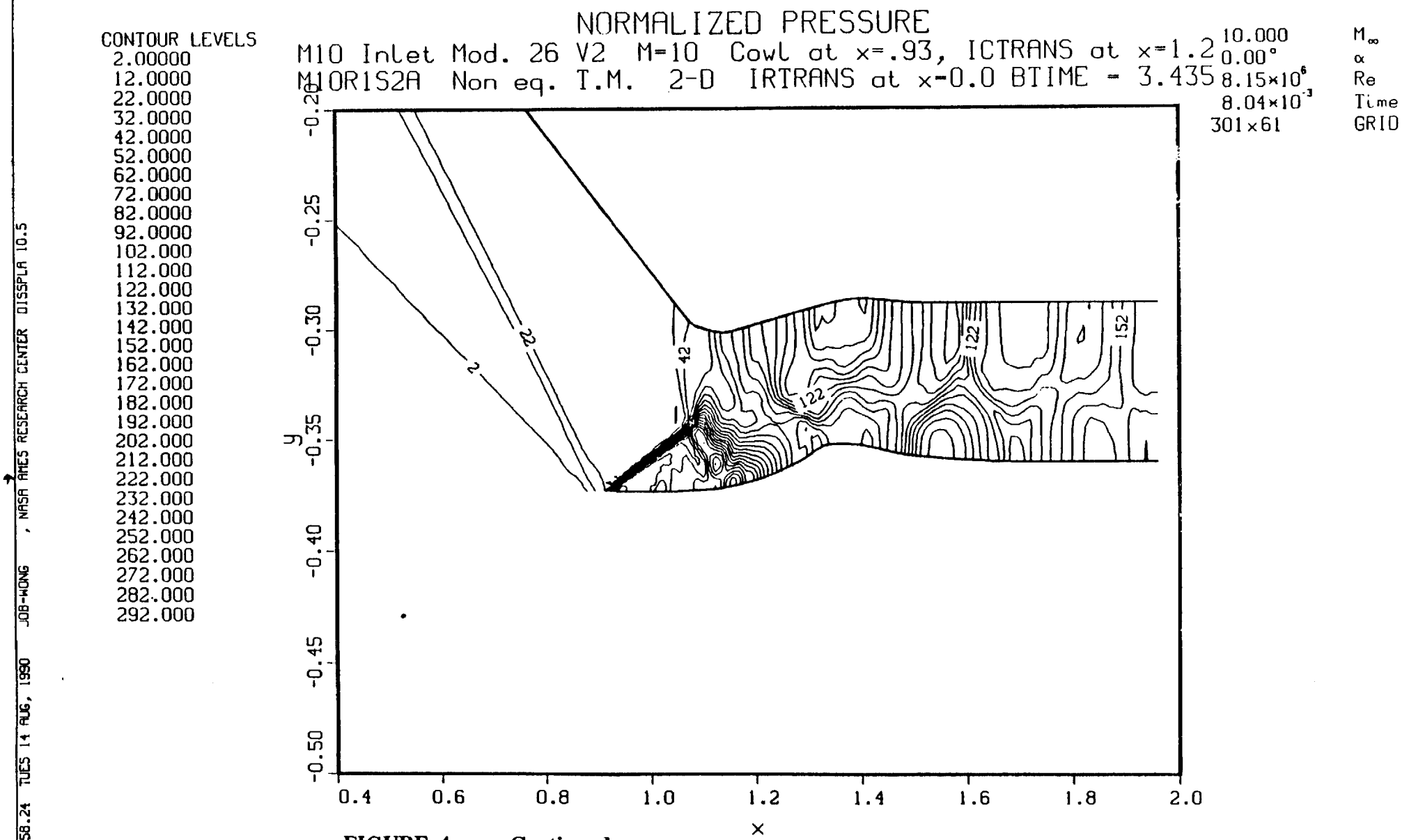

FIGURE 4. Continued.

(b) Pressure contours in throat region.

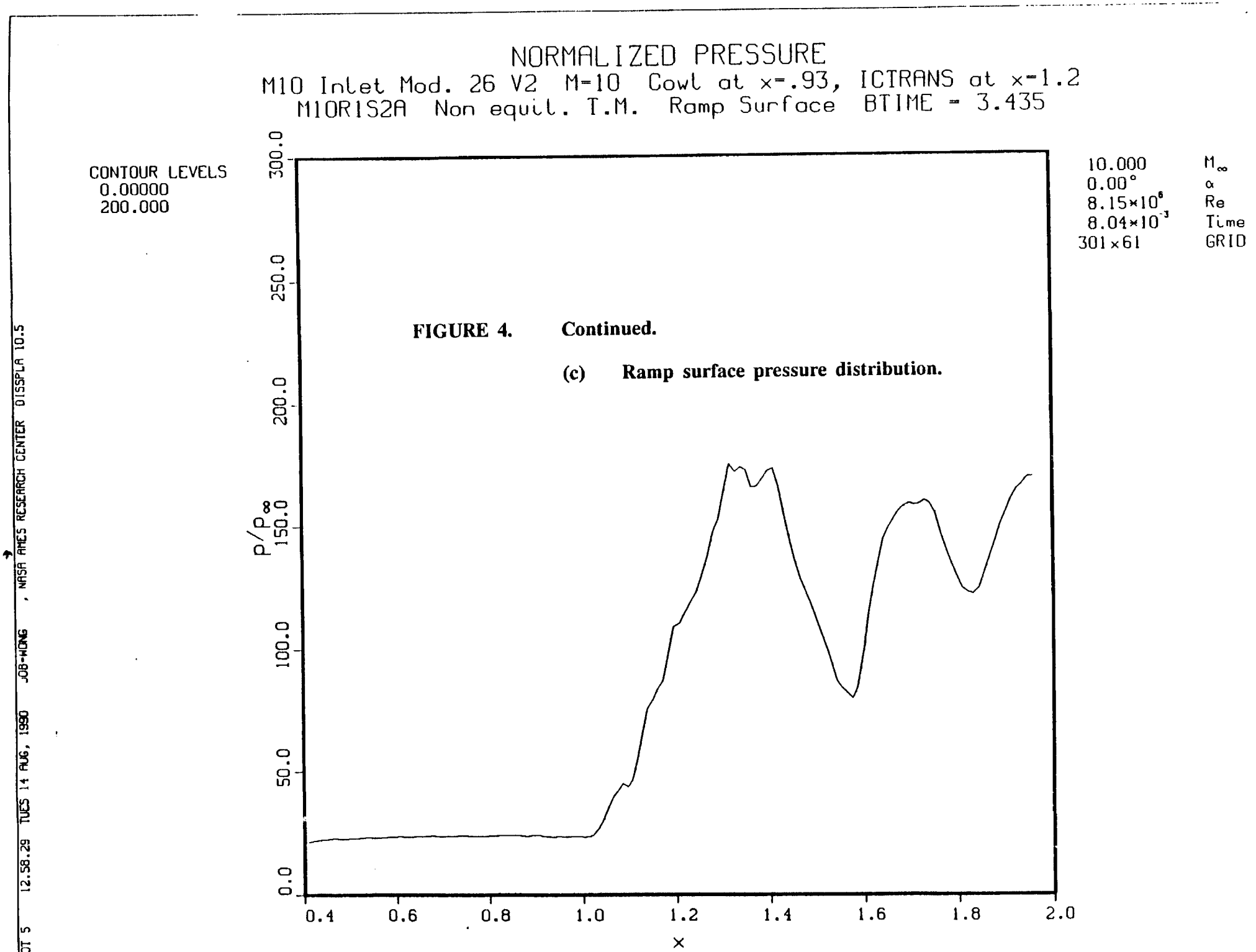

FIGURE 4. Continued.

(c) Ramp surface pressure distribution.

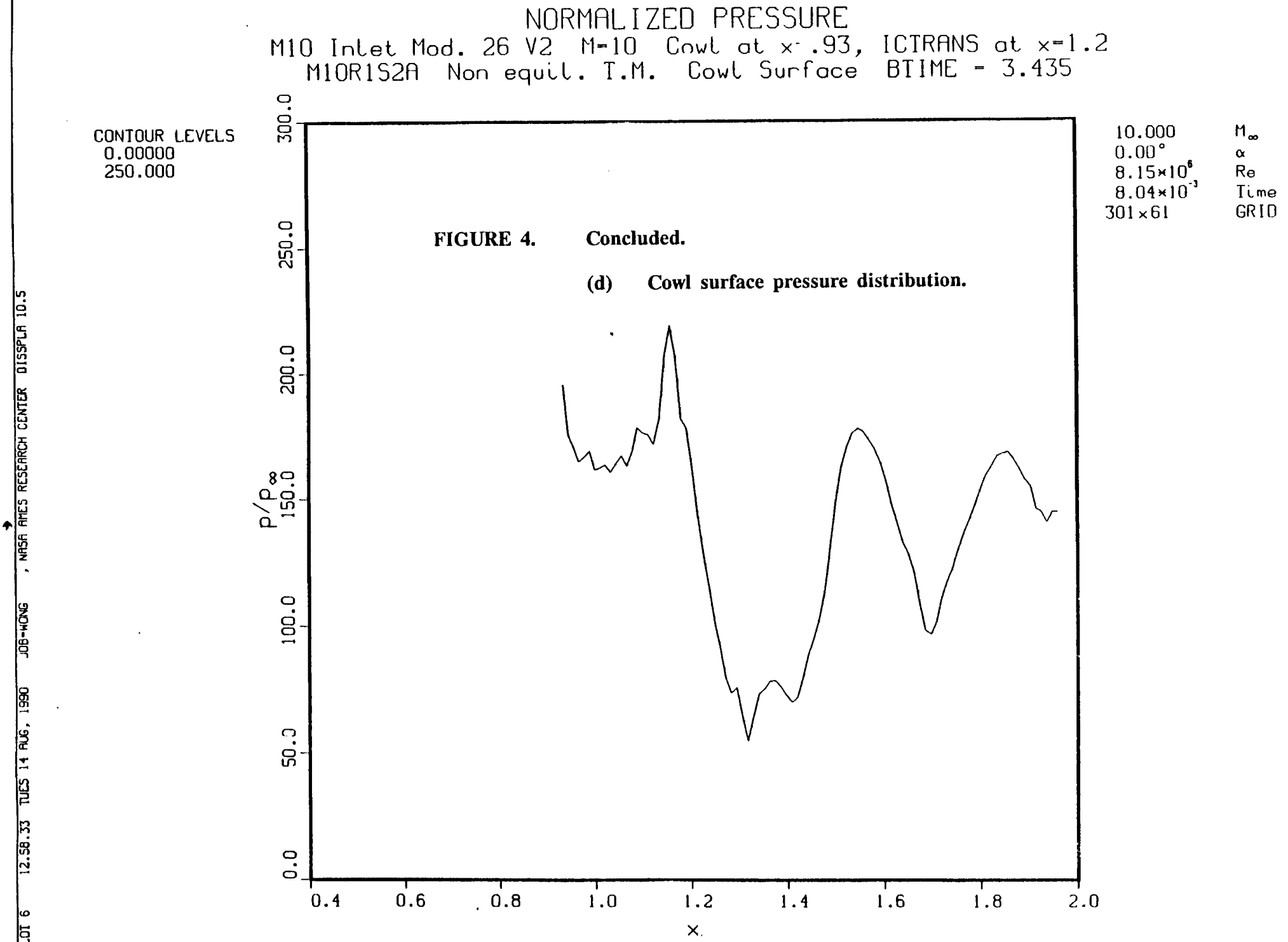

FIGURE 4. Concluded.

(d) Cowl surface pressure distribution.

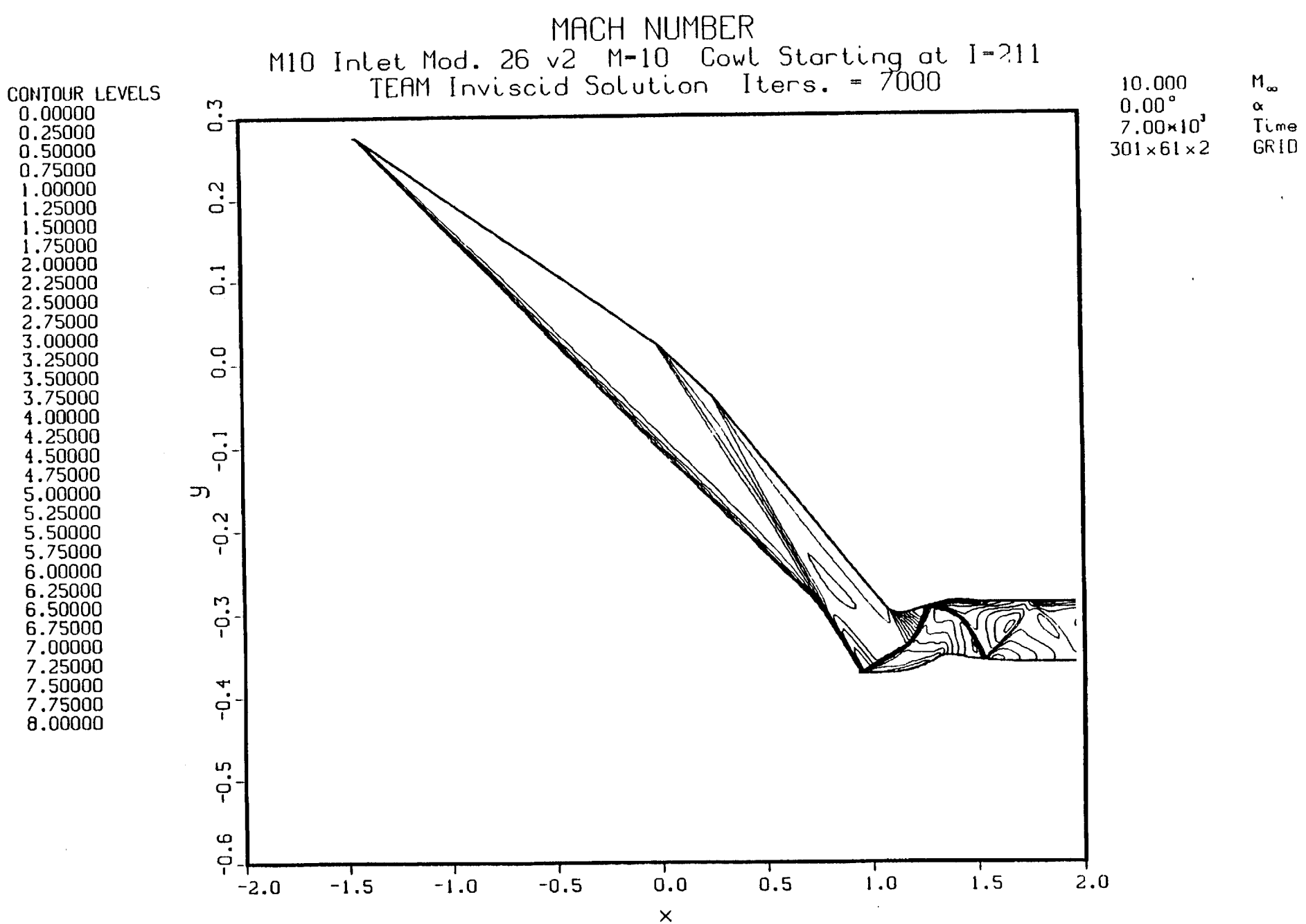

FIGURE 5. **Inviscid flow solution for the inlet with contoured ramp and cowl surfaces at M=10.**

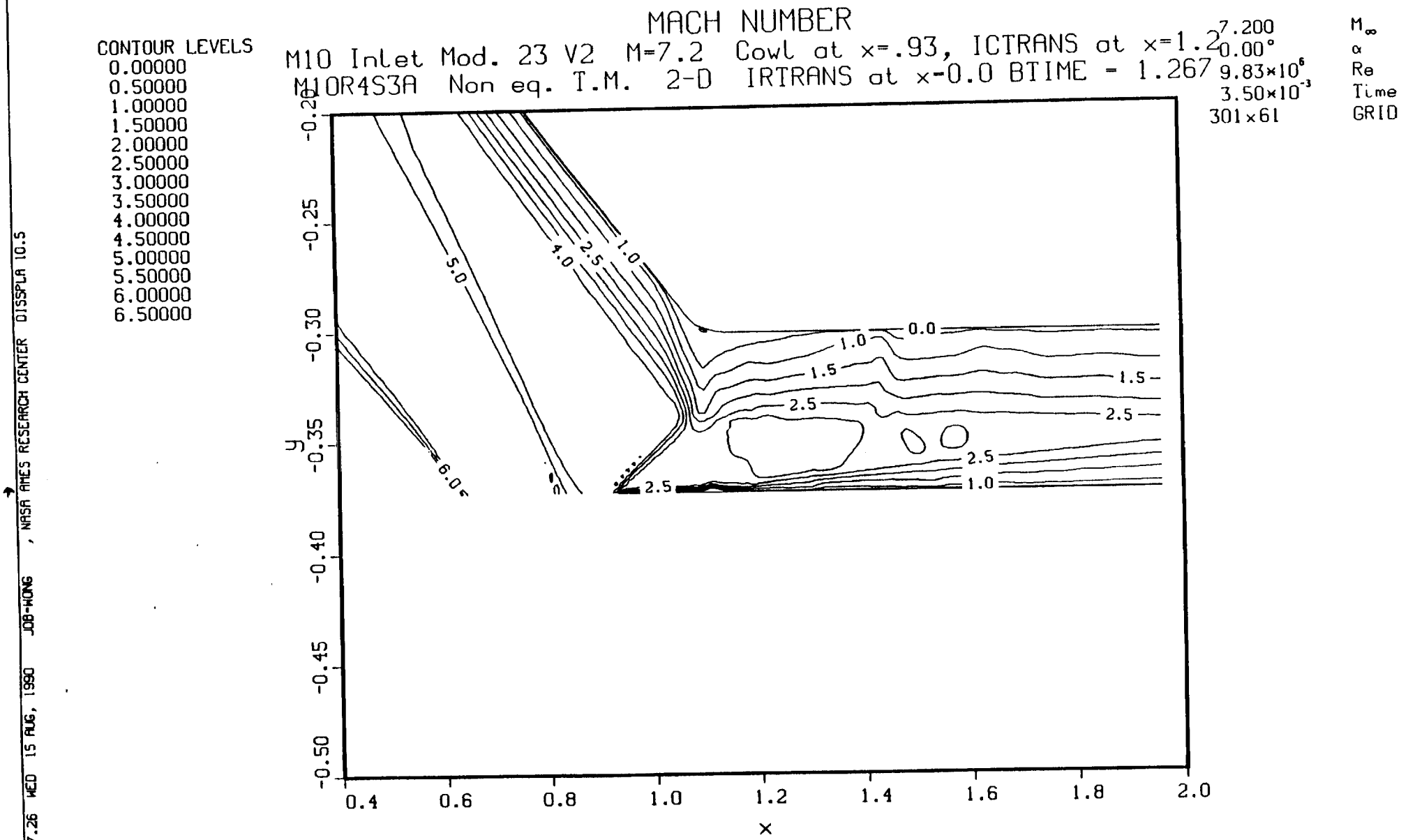

FIGURE 6. **Mach number contours for the straight ramp and cowl geometry at M = 7.2.**

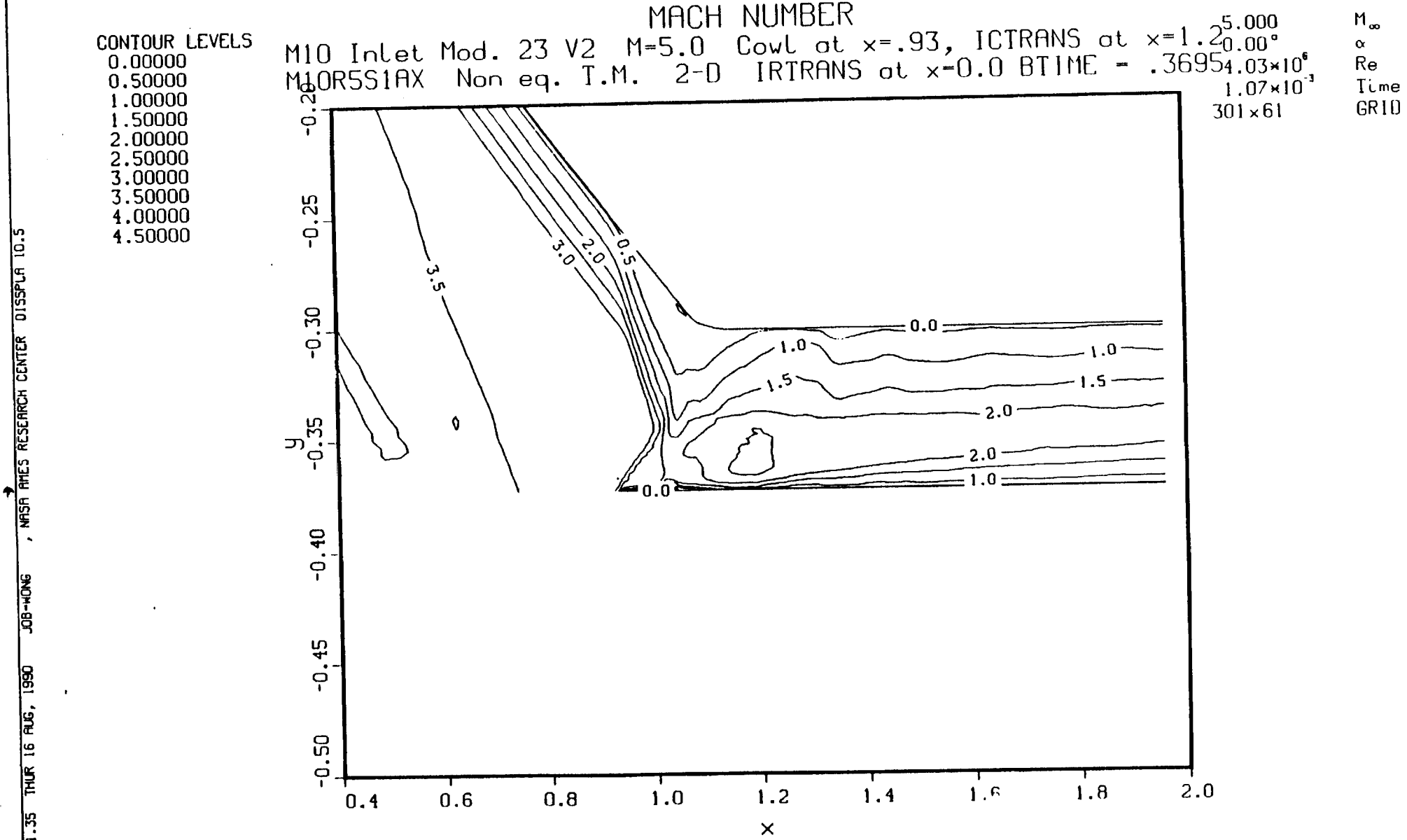

FIGURE 7. **Mach number contours for the straight ramp and cowl geometry at M=5.0.**

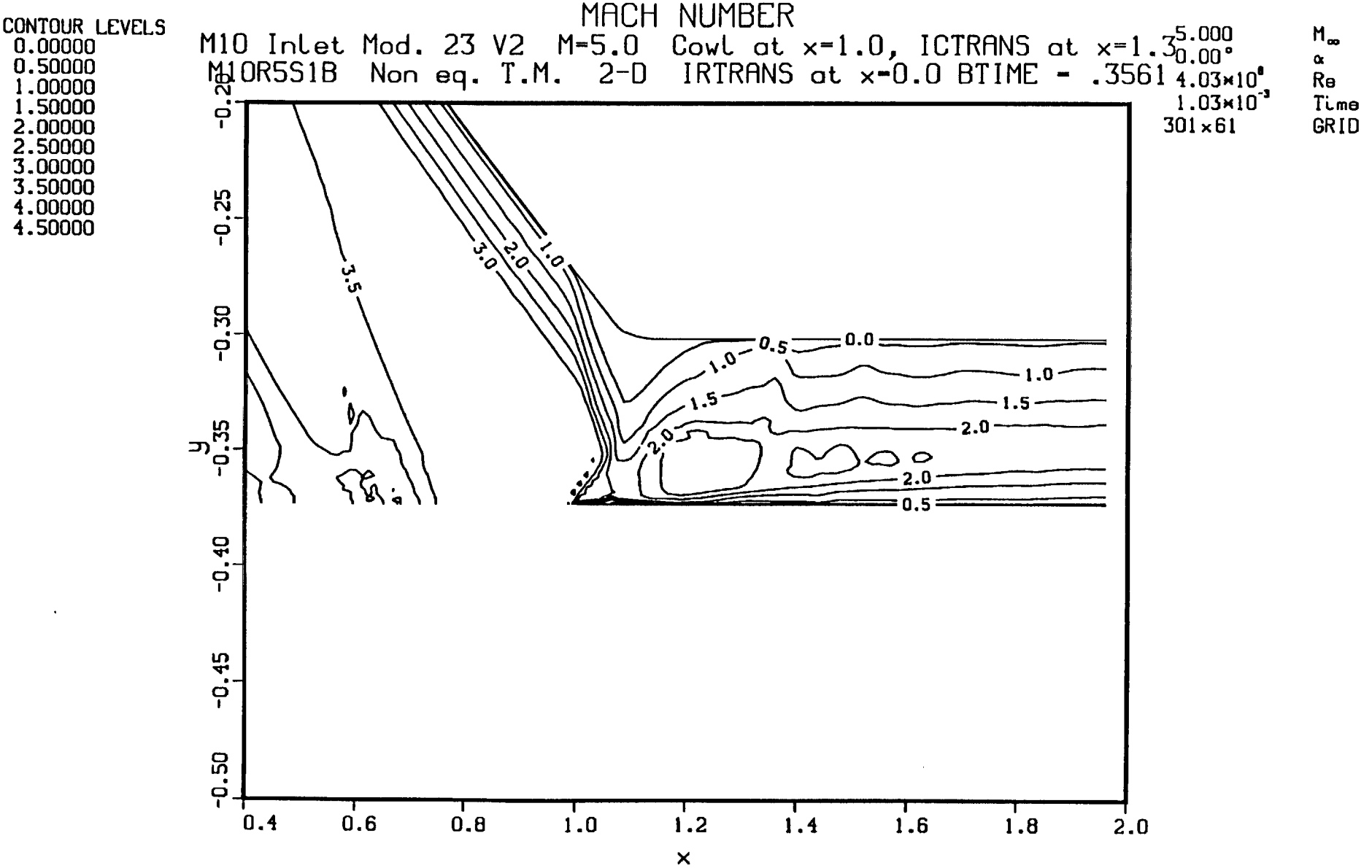

FIGURE 8. **Mach number contours for the straight ramp and cowl geometry at M=5.0 with the cowl retracted.**

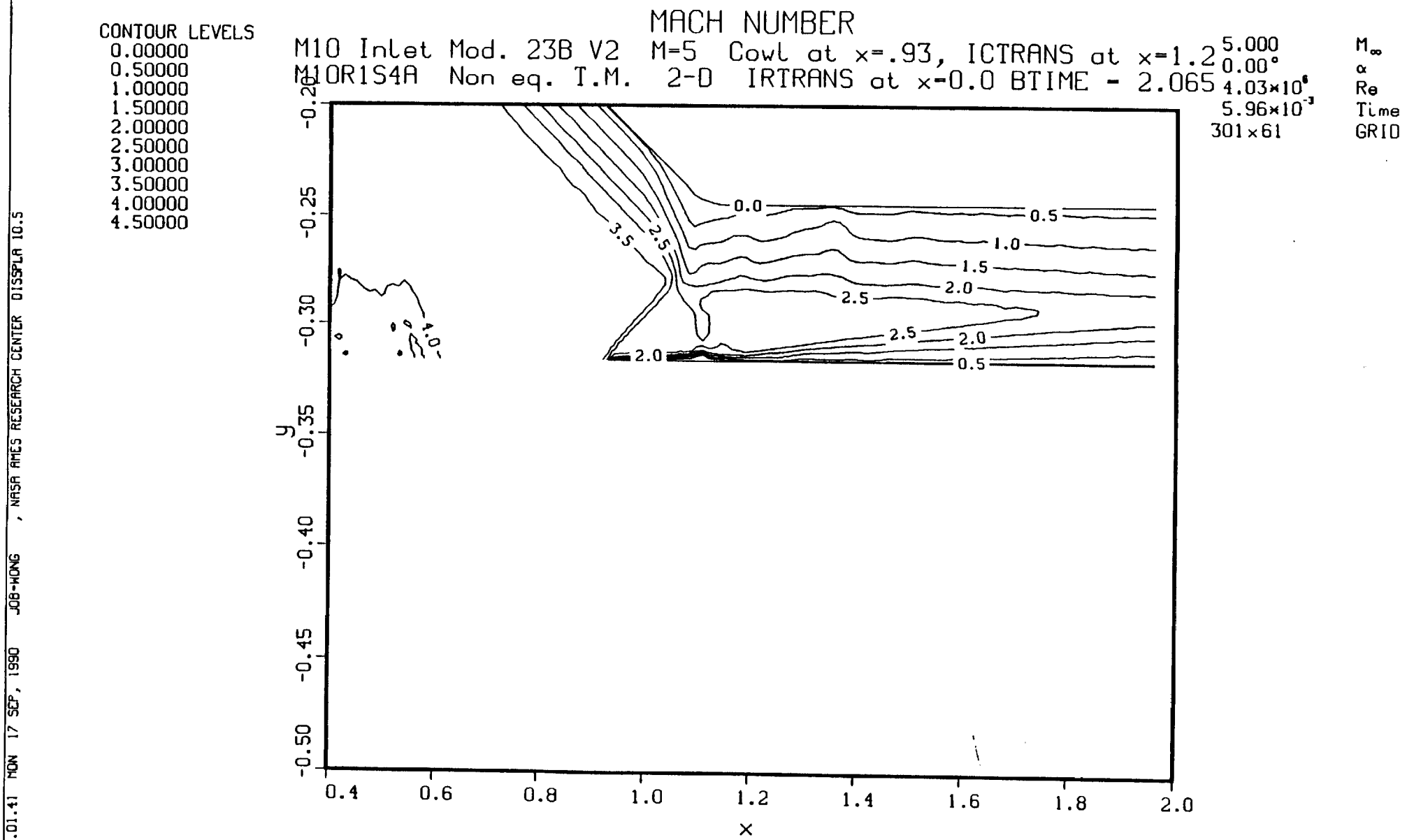

FIGURE 9. **Mach number contours for a 28 degree straight ramp and cowl geometry at M=5.0.**

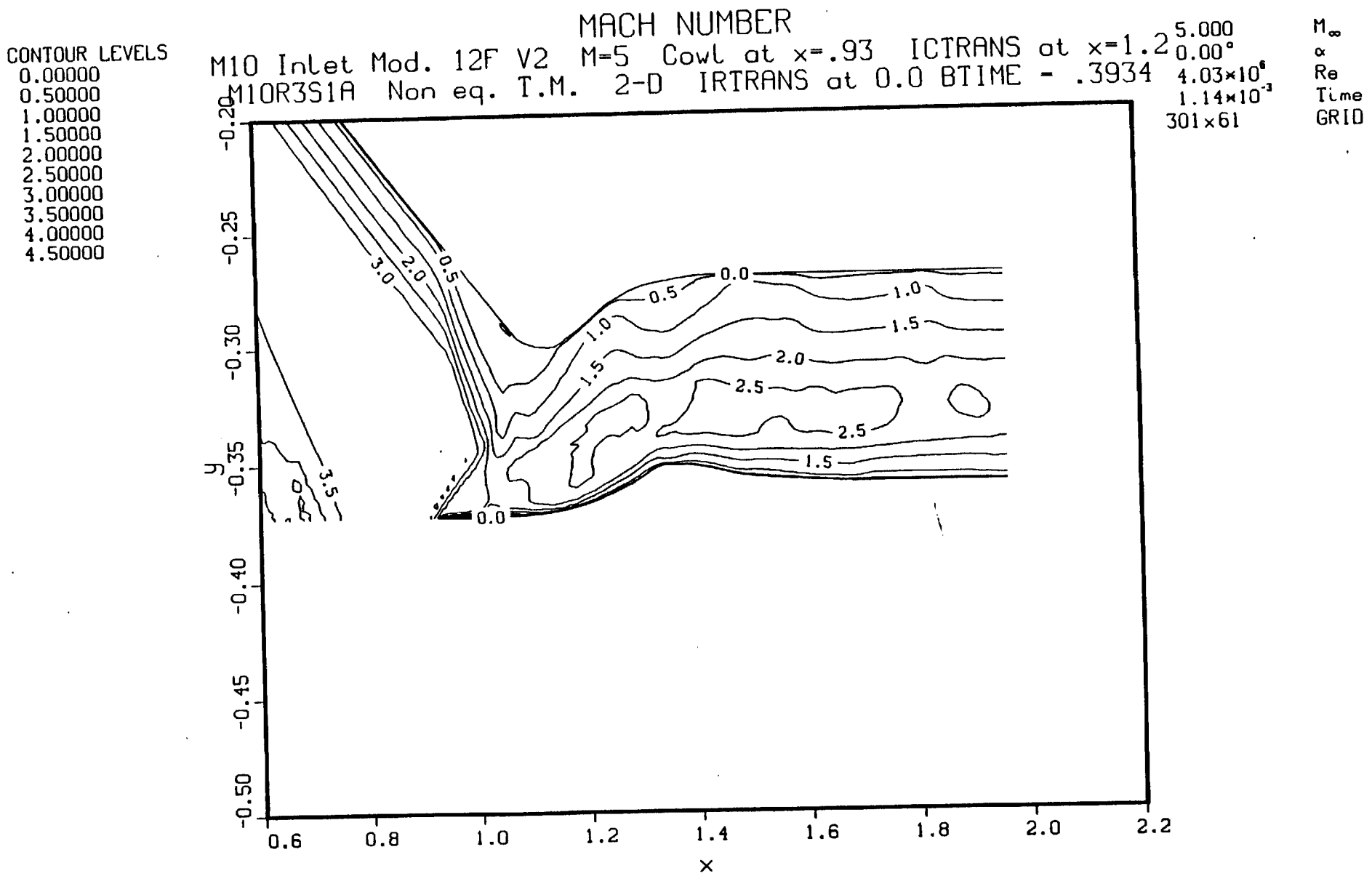

FIGURE 10. **Mach number contours for a 36 degree inlet with a 10 degree expansion in the throat with the cowl forward at M=5.0.**

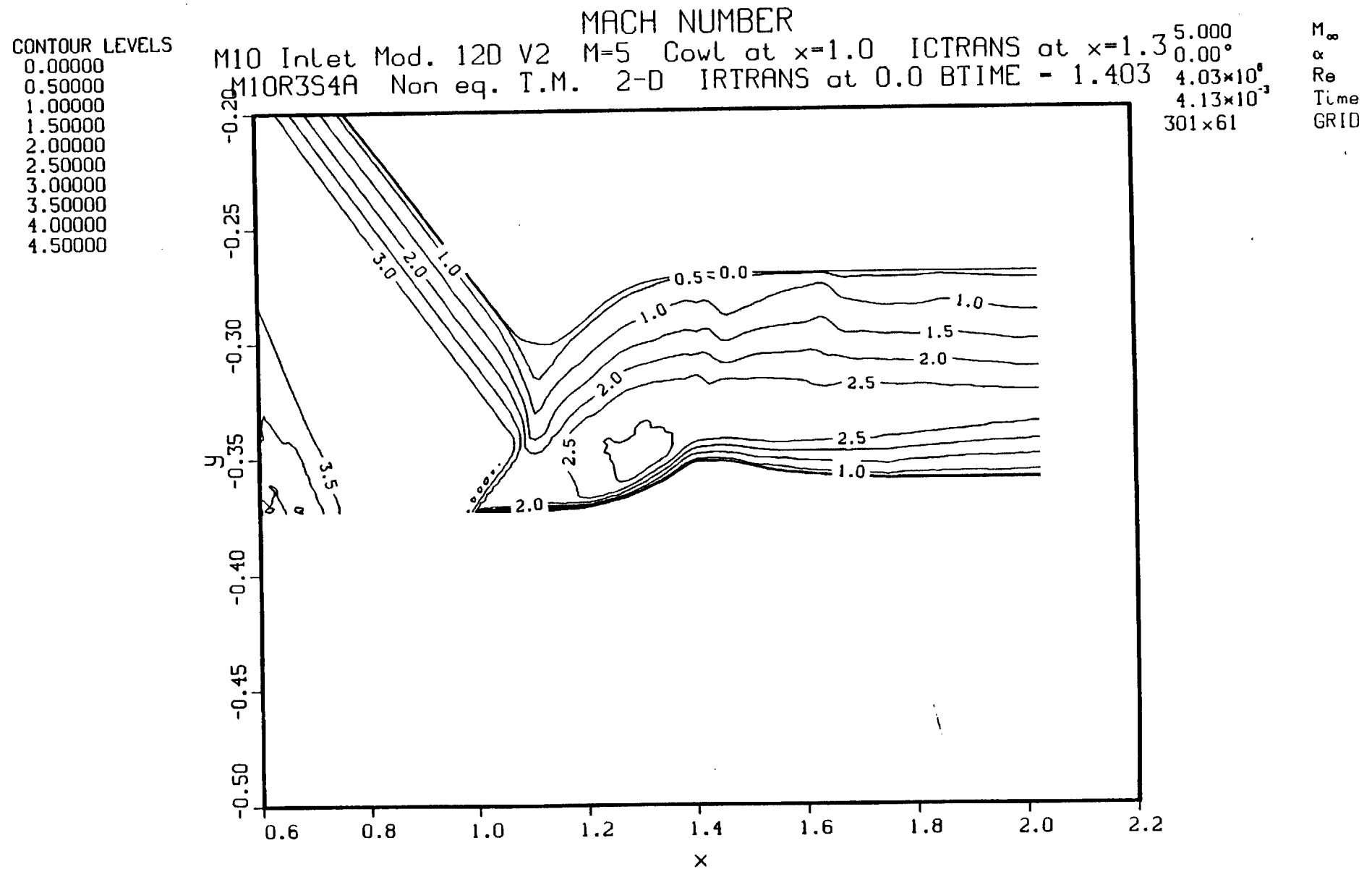

FIGURE 11. **Mach number contours for a 36 degree inlet with a 10 degree expansion in the throat with the cowl retracted at M=5.0.**

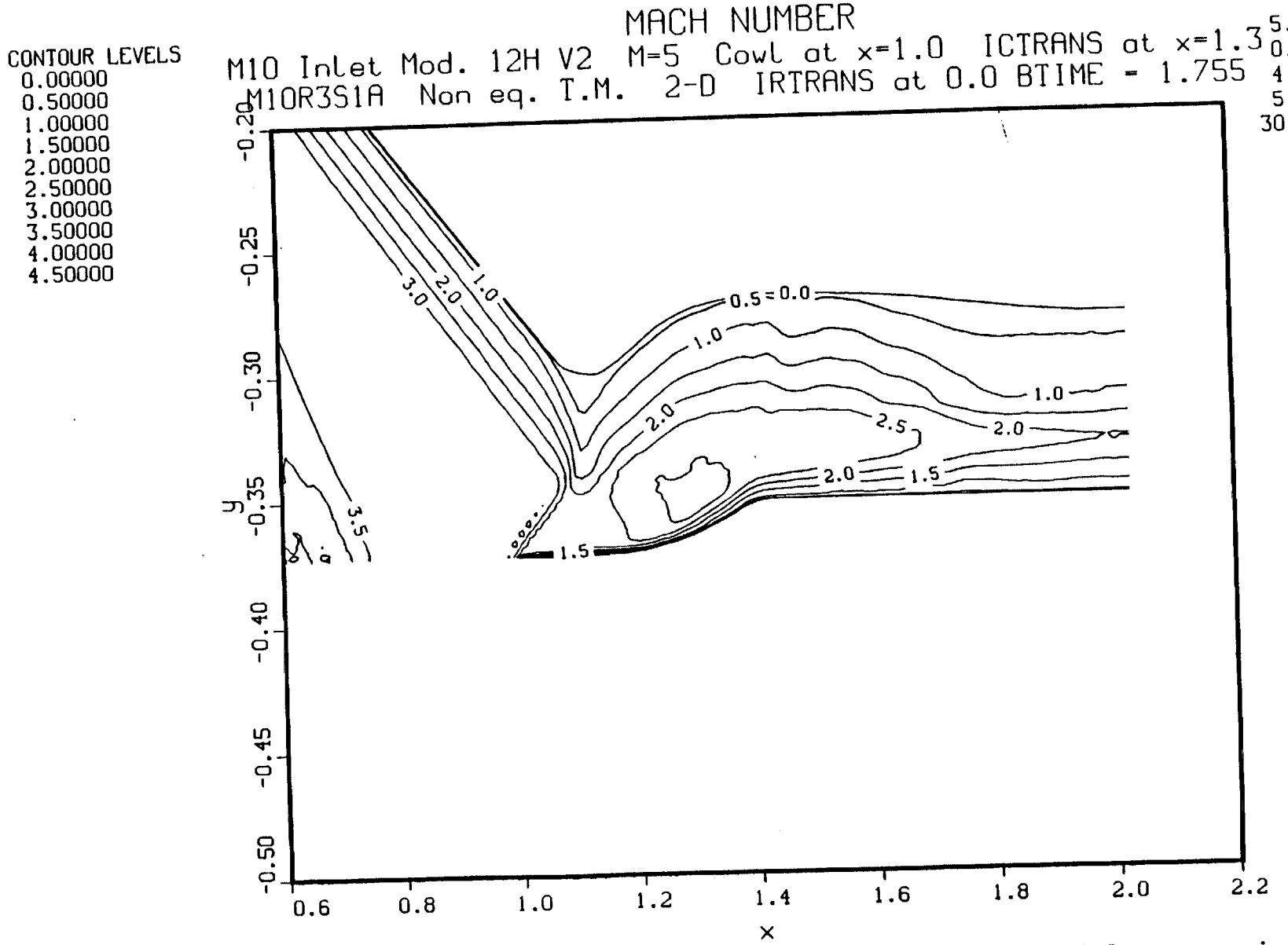

FIGURE 12. **Mach number contours for a 36 degree inlet with a 10 degree expansion in the throat with ramp contouring to achieve additional internal contraction at M=5.0.**

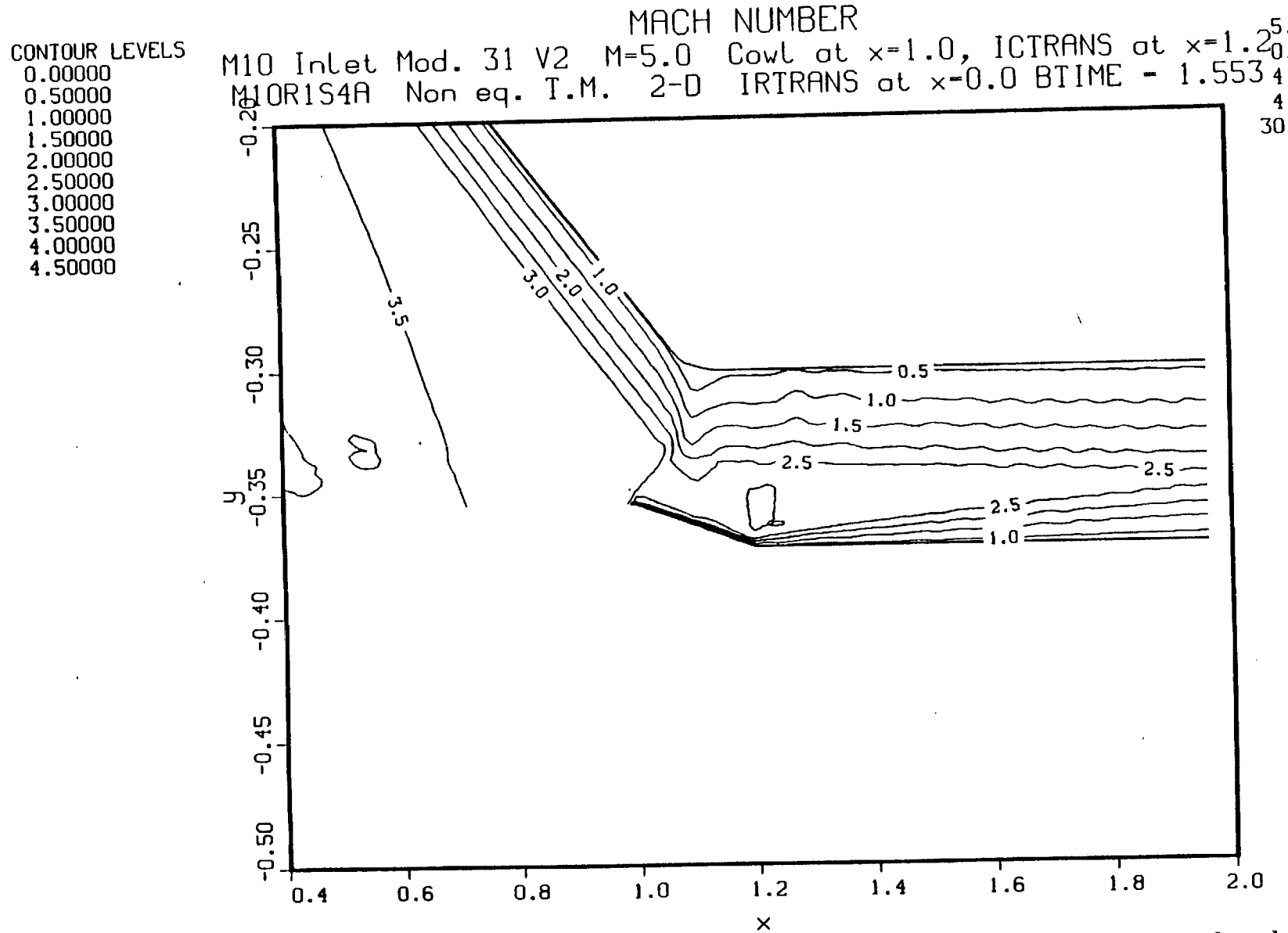

FIGURE 13. **Mach number contours for a 36 degree inlet with a 5 degree drooped cowl at M=5.0.**